

Impact of Gas Solubility on Kick Detection in N-Paraffin Based Drilling Fluids

Leandro Victalino Galves, Federal University of Rio de Janeiro; Roni Abensur Gandelman; André Leibsohn Martins, Petrobras

Copyright 2014, AADE

This paper was prepared for presentation at the 2014 AADE Fluids Technical Conference and Exhibition held at the Hilton Houston North Hotel, Houston, Texas, April 15-16, 2014. This conference was sponsored by the American Association of Drilling Engineers. The information presented in this paper does not reflect any position, claim or endorsement made or implied by the American Association of Drilling Engineers, their officers or members. Questions concerning the content of this paper should be directed to the individual(s) listed as author(s) of this work.

Abstract

There are several technical and environmental aspects that have led the oil industry to increasingly make use of synthetic fluids while drilling. However, such fluids have a capacity to solubilize hydrocarbons present in the drilled formation that hamper the detection of possible unwanted influx into the well. This increases the risk of blowout when the gas kick expands many times its initial volume. Thus, this paper aimed to study the evolution of the gas kick through the well, simulating a blowout condition in view of a transient model. In order to achieve this, a Matlab program was made considering solubility and formation volume factor correlations obtained from the literature, as well as the implementation of a reservoir model, two-phase slug flow and the consideration of the heat transfer from the formation to the drilling fluid. The methane gas was studied in this paper and the drilling fluid was n-paraffin-based. The study demonstrated that when gas starts to come out of solution, the tank gain grows rapidly as does the volume of gas inside the well, leading to a necessity of detecting the kick before it starts to come out of solution. An analysis also showed that it is possible to detect the kick due to the compressibility of the drilling fluid – that made possible to evince a gain in the tank as soon as gas enters the well. The kick took about 49 minutes to be detected in n-paraffin-based fluids and 17 minutes to be detected in water-based systems.

Introduction

Most of the total reserves of oil and gas in Brazil are located offshore in deep-and-ultra-deep-water. In these scenarios, technical problems regarding limited operational windows, high pressures and temperatures, and complications pertaining to well control operations are common. With respect to the technology needed to perform such drillings, the area of study connected to drilling fluids plays a very important role.

Drilling fluids are multiphase systems consisting of water, suspended solids, dissolved salts and organic materials dissolved or emulsified in water or oil. Its functions, among others, involve cuttings transport, balancing the pressures exerted by the formation, wellbore stability, minimizing damage to the formation and cooling and lubricating the bit. They can be grouped in either oil-based or water-based fluids, depending on the type of emulsion they are subjected (direct

or reverse). In drilling operations, oil-based fluids have shown great advantages such as higher lubricity and rate of penetration, and great inhibition of reactivity shales. Nevertheless, the use of such types of fluid has always been linked with high levels of environmental damage. This was a key factor for the upcoming of the synthetic fluids (evolution of conventional oil-based fluids), like n-paraffin.

However, oil-based fluids (synthetic or not), particularly the n-paraffin one, have an ability to solubilize hydrocarbons present in the drilled formation that hampers the detection of unwanted inflows into the well. As a consequence, the kick may migrate through the well from downhole to near the surface, without being detected. At a certain point, as soon as the bubble pressure of the drilling fluid were reached, large volumes of gas would be released in a short period of time, increasing the risk of blowout – gas kicks are highly hazardous because it expands many times its original volume. The behavior of a gas kick in the presence of water-and-oil-based drilling fluids is shown in Fig.1.

With respect to well control, best practices are: first, prevent kicks from happening; second, detecting them as fast as possible, if they occur; and third, control the kick effectively and safely. In addition, monitoring of the parameters of drilling operations provides at least three important parameters for the detection of a kick. These are: pit gain, return flow, and stand pipe pressures.

In view of this, the present work is an application of the knowledge about multiphase flow, PVT models, formation volume factor and solubility correlations, reservoir modeling and temperature gradient. The goal is to study the evolution of a gas kick up in a well, considering a context of blowout. This includes a computer program developed in *Matlab*® which simulates an oil well drilled with n-paraffin-based fluid, suffering a kick of methane gas. The program also aims to assist in monitoring the pressures in the well, as well as identifying the kick through pit gain and increases in the return flow rate.

Literature Review

The study of gas solubility in drilling fluids is relatively recent, dating back to the early 80's. By that time, the focus was to understand the interactions between formation fluids with drilling fluids, considering the pressure and temperature conditions found in the reservoirs.

One of the first works was made by O'Brien [2], who studied gas solubility in oil-and-water-based drilling fluids in light of well control aspects. He concluded that gas solubility in oil-based fluids could be 10 to 100 times higher than in water-based ones. Because of this, pit gain would be small even for large volumes of inflow, delaying the detection of the kick in oil-based systems.

The following year, Thomas et al. [3], continued along the same line of studies of O'Brien [2]. In their research, they used the *Redlich-Kwong* equation of state to calculate the solubility of methane in diesel No. 2. Moreover, with regard to kick detection, Fig. 2 and Fig. 3 show a comparison between the behaviors of pit gain and return flow in oil-and-water-based drilling fluids.

THOMAS et al. [3] concluded that the most reliable indicator of kick during drilling was pit gain. He also affirmed that stopping the mud pumps briefly to check for flow after a drilling break is not a reliable method of kick detection, and that it would take longer in oil-based fluids than in water-based ones.

Later on, O'Bryan [4] extended the studies on oil-based fluids, assessing the factors that affected gas solubility. In his study, he investigated the solubility and saturation pressures of methane in Mentor 28 oil at temperatures of 100 °F, 200 °F and 300 °F. He showed that solubility decreased with increasing temperature or reducing pressure. He also discovered that methane solubility increased by reducing the molecular weight of the oil base and that solids did not have a major role in solubility: 95% of the solubility would occur in the oil phase, while 4.5% in the emulsifier, and 0.5% in the brine.

In 1989, O'Bryan [4] calculated the solubility of methane in oil Mentor at temperatures of 100 °F, 200 °F and 300 °F, using the *Peng-Robinson* equation of state. He proposed a correlation for estimating gas solubility (R_s), according to Eq. 1, where a , b , n and c were constants dependent on pressure, temperature and specific weight of the oil-based fluid.

$$R_s = \left(\frac{P}{a \times T^b} + c \right)^n \quad (1)$$

In 1992, Anfinson and Rommetveit [5] conducted a sensitivity analysis on the performance of important parameters for kick detection, such as pit gain, return flow and stand-pipe pressure. Data were collected from 19 surface and downhole sensors, installed in a 2,020 feet deep exploration well, in which 24 gas kicks simulations were performed. The results showed the necessity of several surface indicators to optimize kick detection and, that pit gain could be very low in oil-based systems. Thus, return flow was the most sensitive parameter in that case. On the other hand, in water-based systems, pit gain and stand-pipe pressure were considered more reliable.

Lastly, Monteiro [1] studied the PVT behavior of n-paraffin-based fluids. He determined and modeled thermodynamic properties of those fluids, such as solubility

and formation volume factor. With the aid of a pressurized PVT cell, the experiments were performed at temperatures of 158 °F, 194 °F and 302 °F. In order to predict the behavior of the gas-drilling fluid mixture during a kick, the softwares *CMG Winprop* and *Labfit* were used. Consequently Monteiro [1] obtained equations for gas solubility (R_s) in n-paraffin-based fluids and formation volume factor (B_f), according to Eq. 2 to 5.

P < 35 MPa:

$$R_{s\ fluid} = 3,486 \times (f_{oil}^{1.306}) \times (P^{1.102}) + e^{0.1019 \times P} \quad (2)$$

$$B_{fluid} = 0,001239 \times (f_{oil}^{1.727}) \times (1,042^P) \times (T^{0.9759}) + e^{0.003981 \times P} \quad (3)$$

35 < P < 50 MPa:

$$R_{s\ fluid} = 0,03401 \times (f_{oil}^{1.296}) \times (P^{2.246}) \times (T^{0.162}) + e^{0.07649 \times P} \quad (4)$$

$$B_{fluid} = 0,001034 \times (f_{oil}^{1.855}) \times (1,076^P) \times (T^{0.8073}) + e^{0.003436 \times P} \quad (5)$$

Computer Program

The program main objective was to be a fast and reliable software for gas kick simulations on wells drilled through formations with abnormally high pressures. Besides, no well control operations subsequent to detection of the influx were to be considered. It was important to study the evolution of the kick without closing the BOP, simulating a blowout scenario which would allow for the prediction of the effect of the kick on two of the most important surface kick indicators while drilling: pit gain and return flow.

Hence, by using a transient model, which considers that the properties being studied vary with time, the program computes: well pressure profile, drilling fluid temperature profile, gas solubility, formation volume factors, kick flow rates, the volume of dissolved gas within the well, the volume of gas coming out of solution, the volume of free gas inside the well, return flow rates, and pit gain. The input data is shown in Fig. 4 and Table 1.

Program Methodology

Hypothesis

Some assumptions were made in order to simplify the computer program and make it feasible from a theoretical-computational standpoint without compromising the credibility of the results. They were: completely vertical well; n-paraffin based drilling fluid; rheology working according to Power Law model; methane gas kick; ideal gas; complete and instantaneous gas solubility in the n-paraffin-based drilling

fluid; insufficient volume of cuttings to change drilling fluid weight or to have any effect on the flow; temperature gradient time independent (but space dependent); free gas pushing drilling fluid above it into the pit; and ROP influent just on kick flow rates.

Methodology

From the input data, the program makes a time-space discretization of the well, creating cells according to the time step defined by the user. Each one of them consists of a volume of fluid within the well in such a way that the sum of the volume of all cells equals the total volume of the well. There is a direct exchange between cell size, computing time, and accuracy with time step. On the one hand, larger time steps increase the cell size allowing for the reduction of computing time, at the expense of accuracy; on the other hand, smaller time steps increase accuracy, but result in computing time growth. As soon as the well is discretized, each computed property will then have a space-time dependent value.

Next step is to calculate the two-phase flow parameters (assuming slug flow), which are dependent on gas holdup. Consequently, if there is no gas inside the well, or all gas is dissolved, gas holdup will be zero, and the “two-phase flow” will become “one-phase flow” instead. Otherwise, the flow will keep being “two-phase”. The pressure gradient is computed in conformity with *Beggs and Brill* correlation [6], Eq. 6. The skin factor was obtained according to Eq. 7 and 8; the two-phase friction factor was found by Eq. 9, f_n by the Moody diagram for smooth tubes, and slug velocity by Eq. 10 [7].

$$\frac{dP}{dz} = \rho_s g \sin\theta + \frac{f_{TP} \rho_n \overline{v_{gofada}}^2}{2(d_2 - d_1)} \quad (6)$$

$$y = \frac{\lambda_L}{H_L(\theta)^2} \quad (7)$$

$$sk = \frac{\ln(y)}{-0,052 + 3,18 \ln(y) - 0,973 [\ln(y)]^2 + 0,0185 [\ln(y)]^4} \quad (8)$$

$$f_{TP} = \exp(sk) * f_n \quad (9)$$

$$v_g = 1,2 \overline{v_{slug}} + 0,35 \sqrt{\frac{g d_n (\rho_L - \rho_G)}{\rho_L}} \quad (10)$$

Subsequently, the program generates a temperature profile of the drilling fluid inside the well assuming it is time independent, as discussed earlier in this chapter. As means to do this, the software *Calor*®, developed by Petrobras, was applied.

Then, summing up the correlations for gas solubility (Eq. 2 and 4), formation volume factor (Eq. 3 and 5), and a reservoir time dependent expression to predict the gas flow into the wellbore (Eq. 11), the volume of dissolved gas, and of gas coming out of solution is measured over time.

$$q_w = (P_i^2 - P_w^2) \frac{2\pi k \cdot ROP \cdot \Delta t}{\ln\left(\frac{4k\Delta t}{\gamma \mu_g \phi c_g r_w^2}\right) * \mu * P_w} \quad (11)$$

Afterwards, conforming to Eq. 12 and 13, developed on laboratory at CENPES/ PETROBRAS, drilling fluid weight, kick weight, and kick flow rate, which had already been estimated previously, are calculated again by means of an iterative process. The values might no longer be the same because dissolved gas might have come out of solution. Thereafter, a loop is restarted and all other variables that were dependent on drilling fluid and kick weight are also recalculated.

Finally, pit gain and return flow rate are evaluated.

$$\rho_{fluid}^{P,T} = \frac{\rho_{fluid}^{std}}{1 + \left(\frac{\rho_{paraffin}^{std}}{\rho_{paraffin}^{P,T}}\right) * f_{oil}} \quad (12)$$

$$\rho_{paraffin}^{P,T} = 8,34 * \frac{141500 + P}{180200 + 212,3T} \quad (13)$$

Pit Gain

Pit gain is the growth of the volume of drilling fluid seen on the surface, above the foreshadowed.

With the purpose of computing the pit gain, it is assumed that dissolved gas that comes out of solution at each time step, pushes the drilling fluid above it into the pit on the surface, making it necessary to estimate how much gas comes out of solution (V_{out}).

Besides, another contribution to pit gain comes from the expansion of the free gas inside the wellbore ($V_{expansion}$); as free gas expands, more drilling fluid is pushed into the pit.

It is also vital to compute the volume of unwanted influx that invades the wellbore every second. However, when it comes to oil-based drilling fluids, it is feasible to consider that all kick solubilizes completely and instantly in the fluid immediately after it enters the wellbore, as long as pressure and temperature conditions allow. Therefore, to an accurate kick detection it is crucial to estimate how a certain amount of drilling fluid expands as gas dissolves in it (V_{in}).

Eq. 14 summarizes all that has been said:

$$V_{pit} = V_{out} + V_{in} + V_{expansion} \quad (14)$$

V_{in} : This portion of the pit gain equation is computed according to Eq. 15 and Fig. 5.

$$V_{in} = V_2 - V_1 \quad (15)$$

Furthermore, it is also important to define a new variable called V_{cel}^{std} . It represents the volume of the fluid-cell on the surface, where all the dissolved gas has already come out of solution. It is noteworthy to mention that $V_{cel}^{std} \neq V_1$ - neither one contains dissolved gas, but V_1 considers the volume variation which occurs to the cell when it is subjected to pressure and temperature conditions of the

well.

To calculate V_2 , Eq. 3 and 5 will be needful. However, such equations are not enough for the precise computation of V_2 . The formation volume factor given by those correlations corresponds to a maximum volume of gas that can be dissolved in the cell. However, if no gas is dissolved in the cell, it is reasonable to assume that $V_2 = V_1$. For this to happen, there is a necessity of creating a correction factor over the mass of gas that dissolves in the fluid-cell, here called $f(m_{gdo})$. Then:

$$V_2 = [B_f * f(m_{gdo})] * V_{cel}^{std} \quad (16)$$

From Eq. 16, we note that the problem of finding V_2 boils down to estimating the value of $f(m_{gdo})$. To this end, it is important to consider the following boundary conditions:

$$\begin{aligned} cc. 1: & B_f * f(m_{gdo} = m_{max}) = B_f \\ cc. 2: & V_2 = V_1 \rightarrow [B_f * f(m_{gdo} = 0)] * V_{cel}^{std} = V_1 \end{aligned}$$

The boundary condition 1 states that if the mass of dissolved gas in the fluid-cell equals to its maximum dissolution capacity, then, formation volume factor is the one given by Eq. 3 and 5. On the other hand, if no gas is dissolved in the fluid-cell, then $V_2 = V_1$. Therefore, approaching $f(m_{gdo})$ by a linear function, we obtain:

$$f(m_{gdo}) = \left(1 - \frac{V_1}{B_f * V_{cel}^{std}}\right) \frac{m_{gdo}}{m_{max}} + \frac{V_1}{B_f * V_{cel}^{std}} \quad (17)$$

Besides, we know that:

$$V_1 = \frac{\rho_{fluid}^{std} V_{cel}^{std}}{\rho_{fluid}^{P,T}} \quad (18)$$

Finally, by replacing Eq. 16 to 18 in Eq. 15, we come to Eq. 19, where $\rho_{fluid}^{P,T}$ is calculated by Eq. 12.

$$V_{in} = \left[\left(B_f - \frac{\rho_{fluid}^{std}}{\rho_{fluid}^{P,T}} \right) \frac{m_{gdo}}{m_{max}} \right] * V_{cel}^{std} \quad (19)$$

V_{out} : The volume of gas coming out of solution per time step is computed by comparing the volume dissolved gas in the cell at an instant of time t , with the amount of dissolved gas in the same cell in an instant $t + \Delta t$. Generically, the volume of gas coming out of solution is given by Eq. 20, and V_1 is obtained by Eq. 18.

$$V_{out} = \left[V_1 R_s \frac{m_{gdo}}{m_{max}} f(t) - V_1 R_s \frac{m_{gdo}}{m_{max}} f(t + \Delta t) \right] \quad (20)$$

$V_{expansion}$: It is the volume expansion undergone by free gas each time step during its flow through the well. As the gas rises, it becomes subjected to lower pressures and temperatures, therefore it expands, in accordance with Eq. 21.

$$V_{expansion} = V(t + \Delta t) - V(t) \quad (21)$$

Assuming the hypothesis of ideal gas, equation of ideal gases can be applied, making it feasible to obtain $V_{expansion}$ by knowing the pressures and temperatures at a time $t + \Delta t$, in agreement with Eq. 22.

$$V_{expansion} = \frac{T(t+\Delta t) P(t)}{P(t+\Delta t) T(t)} V(t) - V(t) \quad (22)$$

RETURN FLOW RATE: Any increase on the return flow rate monitored by surface devices (above the foreshadowed) points that gas is entering the wellbore, or that the existing free gas in the well is in the process of expansion.

Normally, the return flow is an indicator complementary to other kick indicators, such as pit gain. Besides, it is more common to find flowmeters for water-based fluids. Complex conditions of use and compositions create the need for further requirements for the reliability of oil-based fluids flowmeters [5].

In the present work, the return flow rate is simply calculated from the pit gain. Eq. 23 clarifies the way in which the return flow rate is estimated.

$$Q_{return} = \frac{(V_{out} + V_{in} + V_{expansion})}{\Delta t} + Q_{injection} \quad (23)$$

V_{in} , V_{out} and $V_{expansion}$ are found by Eq. 19, Eq. 20, and Eq. 22, respectively.

Results

The most important results are shown in two parts: in the first one, there is a description of the outcome of the simulations on the standard-scenario studied; in the second, a sensitivity analysis determined the influence of oil fraction, drilling fluid rate and kick flow rate on kick detection, considering either pit gain or return flow.

Standard Scenario

The so-called *standard-scenario* was planned with clear intention of examining a situation close to those found in actual deep-water drillings. This is important because of the new trend of application of n-paraffin-based fluids in the pre-salt. The input data (well geometry and characteristics of the reservoir and drilling fluid) is mentioned in Table 1 and Fig. 4.

The results are presented below:

The pressures encountered in the well, exhibited in the Fig. 6, indicate the existence of four distinct regions defined by depth. Such occurrence is justified due to different hydraulic diameters of the well. Region 1, where the lowest pressures were seen, refer to the riser; the second designates the whole area filled by the 9 5/8 casing; the third is characterized by the presence of barefoot well and no drill collars in the drill string; and the fourth corresponds to the "end" of the well, where it is opened to the formation and

there are drill collars. In region 4, the highest pressures were recorded. They reached almost 10,000 psia – numbers seen only in very deep wells.

Figure 7 shows the temperature profile of the drilling fluid. The curve was generated by the software *Calor*®, licensed by Petrobras. According to Fig. 7, the temperature reached around 110 °F (43 °C) in greater depths, while when the fluid caught up the riser, its temperature reduced to less than 40 °F (4 °C).

The variation of gas solubility with depth is shown in Fig. 8. It is possible to observe the enormous capacity of the n-paraffin-based drilling fluid to dissolve gas. The curve was generated by gas solubility correlations from [1] (Eq. 2 and 4). The discontinuity present in the graph is caused by the use of two different expressions to cover the entire range of pressures studied here. Monteiro [1] did not foresee any equation for pressures greater than 7,252 psia; therefore, it was necessary to extend the use of those equations to upper limits.

Fig. 9 pictures the results for another important property of the drilling fluids when it comes to kick detection calculations: formation volume factor. In line with this graph, the formation volume factors found downhole indicates the high volume variation to which the fluid is subjected under the presence of a certain mass of dissolved gas. The expansion of a given volume of fluid as it dissolves gas is important to the detection of the kick before the gas starts to come out of solution – according to Fig. 9, a fluid-cell downhole would more than duplicate its volume if all its gas dissolution capacity was used.

To analyze the graph of Fig. 10, it is worth dividing it into three regions: left, middle and right. Left region is characterized by the slow growth of the amount of dissolved gas. That is explained due to low kick flow rates in the beginning of the kick (in line with Fig. 15). However, it is also possible to see that this growth is accelerating (positive derivative). In the middle region, such growth has become proximately constant as the “contaminated” cells (the ones containing dissolved gas) flows from downhole towards the surface. In the right region, the growth acceleration becomes negative (negative derivative) and the curve changes the slope. That indicates that the well is completely filled with “contaminated” cells. It is noteworthy to mention that there will always be growth on the volume of dissolved gas, because the kick flow rate is always increasing.

It can be noted from the graph of Fig. 11, that the accumulated volume of gas coming out of solution and the volume of dissolved gas (Fig. 10) have the same order of magnitude, as expected. It is also worth noting that it has taken about 3 hours for dissolved gas to start to come out of solution. From the point where the well starts to present free gas, the curve of Fig. 11 grows rapidly.

The graph of free gas, exhibited in Fig. 12, represents one of the most important results that the program provides. It is vital not only for the calculation of pit gain, as is it also essential to estimate the return flow. It differs from Fig. 11 because it corresponds to a volume of free gas which matches the state of the well at a certain moment and not the

accumulated volume of gas at surface conditions. Therefore, the discrepancy with respect to orders of magnitude is very big. Along the study period, the amount of free gas within the well reached over 700 barrels; however, in Fig. 11, it is known that a much greater volume of gas had already come out of solution (and had seeped out from the well). By the graph of Fig. 12, the gas started to come out of solution after 3 hours from the beginning of the kick.

Fig. 13 and 14 show the results regarding to kick detection in the standard-scenario studied here.

Finally, the pit gain (Fig. 13) and the return flow (Fig. 14) indicated the time interval from the starting of the kick to its detection. A comparison was also made with the same time found in drillings which make use of water-based fluids.

To define a criterion of minimum equipment sensitivity for kick detection in the field, it has been established that a pit gain of 15 barrels and an increase of 5% in the return flow rate were feasible numbers (i.e. 420 gal/min in the standard-scenario).

Thus, according to pit gain (Fig. 13) the kick would be identified in 1,015 sec (~ 17 minutes) if a water-based fluid was used, whereas the return flow stated that the same would be identified in 1320 sec (~ 22 minutes). On the other hand, detection in n-paraffin-based drilling fluids were considerably slower, as expected. The pit gain detected the *kick* in 2960 sec (~ 49 minutes) and the return flow took 14790 sec (~ 4 hours) to realize the 5% increase.

Sensitivity Analysis

The sensitivity analysis was made in an attempt to study the effect of a variation of oil fraction, drilling fluid rate, and kick flow rate on kick detection.

Tables 2 to 4 evince the time to an increase of 15 barrels of fluid in the pit, and to 5% and 1% increases in the return flow. Also, it was included in these tables (at the rightmost column), the minimum sensitivity that return flow equipment should have to be a kick indicator with similar efficiency to pit gain.

OIL FRACTION: Table 2 shows the results for oil fractions of 46%, 60% and 78%. These fractions are the same considered by Monteiro [1] to find the correlations of gas solubility and formation volume factor used in this work.

From the figures presented in Table 2, we can note a curious situation. The increase in the oil fraction plays an opposite role on kick detection when measured by pit gain and when estimated by the increase in the return flow. On the one hand, with regard to return flow, the growth in the oil fraction raises the time to kick detection. That is because large increments in the return flow are connected to gases (dissolved) coming out of solution. As a consequence, it is expected that the higher the oil fraction, the higher the capacity of a fluid-cell to dissolve gas; therefore, the cell would become saturated later and gas would come out of solution with some delay, causing the return flow to grow later as well - for fractions of 78%, the gas took almost four hours to start to come out of solution (very close to the surface

already, considering that a cell takes approximately 4.6 hours to go from downhole to the rig); for fractions of 60%, the gas took proximately 3 hours; and for fractions of 46%, the gas took less than 2.3 hours to come out of solution. On the other hand, when considering pit gain, the increase in the oil fraction resulted in decrements of the time to kick detection. This happened due to an unbalance between the growth of gas solubility and formation volume factor – gas solubility increases slower than formation volume factor as the oil fraction becomes higher. Besides, both are very important to compute pit gain, as stated in Eq. 15, 19 and 20. As kick flow rates are initially low, and no gas comes out of solution before the detection of 15 barrels (average detection time was 49 minutes, while dissolved gas would only come out of solution after more than 2,3 hours), it was expected that the change in oil fraction, within the studied range would not be significant enough to promote any variation in the time to kick detection, since kick flow rate does not vary with oil fraction; however, the fast growth of the formation volume factor resulted in a faster perception of the same 15 barrels. That might be occurring due to the use of Monteiro [1] correlations outside the pressures range foreseen by him. Thus, the analysis of the influence of the oil fraction on pit gain might be showing inconclusive result.

Furthermore, another point to be considered from the analysis of the data in Table 2: is that once again the return flow is less efficient to kick detection than pit gain. To make the return flow equally efficient as pit gain, its minimum sensitivity to perceive small increases should be of 1% in water-based fluids and 0.1% in n-paraffin-based fluids.

DRILLING FLUID RATE: **Erro! Fonte de referência não encontrada.** shows the influence of different drilling fluid rates on kick detection. Three different flow rates were analyzed: 250, 400 and 600 gal/min. Those flows were considered low, medium and high, respectively.

According to **Erro! Fonte de referência não encontrada.**, the higher the drilling fluid rate, the higher the time to kick detection for both n-paraffin-and-water-based fluids. This result becomes more intuitive when we think that if the drilling flow rate was zero, it would be even quicker to detect the kick, since, due to lack of circulation of fluids within the wellbore, more gas would accumulate, leading to a faster increase in the fluid level of the drilling fluid tank.

By examining the return flow on kick detection, it is expected that it has the same trend of pit gain to identify the kick faster when drilling fluids rates are low. This behavior is seen for the water-based fluid. However, in the n-paraffin-based fluid, such tendency is viewed only when the flow rate goes from 250 to 400 gallons per minute. As the flow rate reaches 600 gallons per minute, it is already so high that the circulation of fluids inside the well occurs fast enough to avoid too much of gas accumulation. Furthermore, high drilling fluid flow rates are related to higher dynamic pressures; then, reduced kick flow rates; and consequently, gas coming out of solution later.

Besides, once more, the average time to kick

detection in the n-paraffin-based fluid was about 3 times greater than that for the water-based fluid.

KICK FLOW RATE: Figure 15 illustrates the different curves considered during the simulations for the sensitivity analysis of this parameter. High or low kick flow rates were obtained by varying the formation pore pressure. They were named: very low flow rates (curve 1), low flow rates (curve 2), mean flow rates (curve 3) and high flow rates (curve 4), according to their inclinations: the more horizontal, the lower; otherwise, the more vertical, the higher.

Table 4 shows the results for kick detection by different kick flow rate curves.

A close examination of the figures in Table 4 conveys that increases in kick flow rate imply some sort of reduction in the time to kick detection. It is expected that if a greater volume of gas influx per time invades the wellbore, the pit gain and the return flow will rise faster. A keen observer could argue that the soon detection of the kick could also imply larger volumes of gas into the well, since kick flow rates would be higher. However, as shown in Table 4, the quick detection compensates the lofty kick flow rates. Thus, less gas ends up invading the well. This leads us to conclude that higher kick flow rates are less harmful in terms of "kick size" than small flow rates, at least until the identification of the unwanted influx (for both types of fluids).

Another important finding is that gas volumes from 10 to 20 times greater are associated with n-paraffin-based fluids (until kick detection) when compared to water-based fluids.

Conclusions

- The study demonstrated that kick detection in n-paraffin-based fluids is slower than in water-based fluids, indeed. In the scenario analyzed, the kick was detected in 17 and 49 minutes for water-based and n-paraffin-based fluids, respectively. That is, a pit gain almost 3 times slower comparing water base with n-paraffin base. In addition, the return flow was shown to be less reliable for identifying a kick, as it realizes the kick later compared to pit gain: 22 minutes for the water-based fluid, and 4 hours for the n-paraffin-based fluid. Due to this occurrence, the return flow would only exhibit the same efficiency as pit gain if it could be sensitive enough to detect increases of 1% if the drilling fluid was water-based and 0.1% if it was n-paraffin-based.
- The sensitivity analysis supported that reductions in the drilling fluid rate would be beneficial for faster kick detection, whereas decreases in the values of kick flow rate induced a delay to identify the unwanted influx. In addition, small kick flow rates would not outweigh the additional seconds of exposure to it, being connected to higher volumes of gas entering the wellbore. Contrarily, for high kick flow rates, the kick would be perceived much faster. In this last case, just relatively little gas would have invaded the wellbore until detection. With respect to the volume of gas that enters the well before detection, 10 to

20 times more of it is linked to n-paraffin-based fluids in comparison with water-based fluids.

- *Oil fraction* was the protagonist of a curious case: the more n-paraffin was mixed in the drilling fluid, the greater the time to kick detection by the return flow, yet, the lower was it considering the pit gain. The explanation for this goes through the use of Eq. 3 and 5 to compute the formation volume factor profile, which was very sensitive to changes in the oil fraction. These equations were employed outside the pressure ranges for which they were made, according to [1]; therefore, it is understandable that these calculations show some irregularity.
- Finally, despite all the problems of slow kick detection in n-paraffin-based drilling fluids, once they were detected, engineers would have more time to act upon well control than if water-based fluid was being used. In the scenario analyzed, they would be provided 64 minutes to act before the blowout (i.e. gas breaking out at the surface) and only 33 minutes if the fluid was water-based. Therefore, since flowmeters and equipment to measure pit gain were sensitivity enough to detect small increments - 15 barrels or less of pit gain and 0.1% increase in the return flow - and other kick indicators could serve as allies, as for example, reducing the drilling fluid rate to see whether the well would flow, there is little reason not to use, or to fear, n-paraffin-based drilling fluids when it comes to kick detection.

References

1. MONTEIRO, E. N., "Estudo do Comportamento PVT de Misturas de Metano e Fluidos de Perfuração Base N-Parafina", Tese de M.Sc., Unicamp, Campinas, SP, 2007.
2. O'BRIEN, T. B., "Handling Gas in an Oil Mud Takes Special Precautions", *World Oil*, pp. 22-29, 1981.
3. THOMAS, D. C., LEA JR., J. F., TUREK, E. A., "Gas Solubility in Oil-Based Drilling Fluids: Effects on Kick Detection", *SPE 11115 - SPE 57th Annual Fall Technical Conference and Exhibition*, pp 26-29, New Orleans, LA, Sep. 1982.
4. O'BRYAN, P. L., "Well Control Problems Associated with Gas Solubility in Oil-Based Drilling Fluids", PHD, Louisiana State University, LA, 1989.
5. ANFINSEN, B. T., ROMMETVEIT, R., "Sensitivity of Early Kick Detection Parameters in Full-Scale Gas Kick Experiments with Oil- and Water-Based Drilling Muds", *IADC/SPE 23934 - IADC/SPE Drilling Conference*, pp 18-21, New Orleans, LA, Feb. 1992.
6. BEGGS, H. D., BRILL, J. P., "Two-Phase Flow in Pipes", 6 ed. Tulsa, OK, University of Tulsa, 1978.
7. NICKLIN, D.J., WILKES, J. O., GREGORY, G. A., "An Intermittent Two-Phase Flow in Vertical Tubes", *Trans. Inst. Chem. Eng.*, pp. 61-68, 1962.

Tables

Table 1. Input data.

Gravity	9,81 m/s ²
Surface Temperature	59,00 °F
Atmospheric Pressure	14,70 psia
Consistency Index	2,72 Pa.s ⁿ

Behaviour Index	0,60
Drilling Fluid Weight at the Surface	10,00 ppg
Pure Paraffin Weight at the Surface	6,40 ppg
Gas Kick Weight Downhole	2,00 ppg
Drilling Fluid Rate	400,00 gal/min
Oil Fraction	0,60
Rate of Penetration (ROP)	10,00 m/h
Kick Viscosity	0,03 cp
Reservoir Permeability	30,00 mD
Reservoir Porosity	0,20
Euller Constant	1,78
Time Step	20,00 s
Study Period	5,00 h

Table 2: Analyzed parameter: oil fraction.

Oil Fr. (%)	Pit gain - 15 bbl (s)	Increase in the return flow (s)		Minimum sensitivity (%)
		5%	1%	
78	2700	15500	14300	0,1
60	2960	14790	13000	0,1
46	3190	13400	11300	0,1
Water-Based	1015	1320	1015	1

Table 3: Analyzed parameter: drilling fluid rate. Blue: oil-based fluid; red: water-based fluid.

Drilling fluid rate (gal/min)	Pit gain- 15 bbl- (s)	Increase in the return flow (s)		Minimum sensibility (%)
		5%	1%	
250	2875	14700	11400	0,2
400	2960	14790	13000	0,1
600	3005	*	10400	0,1
250	890	950	830	2,3
400	1015	1320	1020	1
600	1170	2220	1255	0,5

* Flows 5% higher than 600 gal/min were not reached during the study period.

Table 4: Analyzed parameter: kick flow rate. Blue: oil-based fluid; red: water-based fluid.

Kick Flow Rate Curves	Pit Gain 15 bbl- (s)	Total vol. of influx before detection (stb)	Increase in the return flow (s)		Minimum Sensitivity (%)
			5%	1%	
Curve 1	5270	192200	*	*	0,1
Curve 2	3660	134000	15740	15180	0,1
Curve 3	2960	109400	14790	13000	0,1
Curve 4	2550	95485	13360	11280	0,1
Curve 1	1090	9539	1340	1060	0,9
Curve 2	1040	8944	1325	1020	1

Curve 3	1015	8860	1320	1015	1
Curve 4	990	8606	1270	970	1

* Flow rates of 5% and 1% greater than 400 gallons per minute were not reached during the study period, when the kick flow rate was deemed too small.

Figures

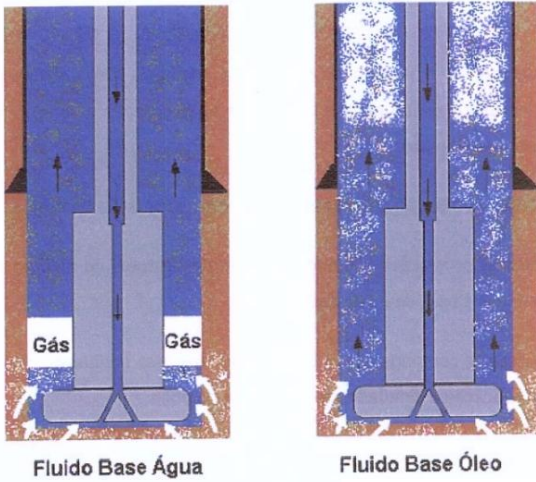


Fig Water Based Fluid 1 water Oil Based Fluid muds [1].

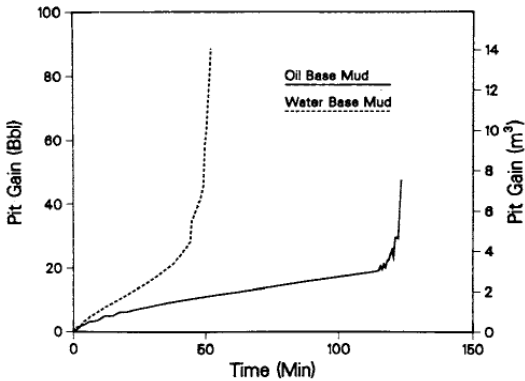


Figure 2. Pit gain [3].

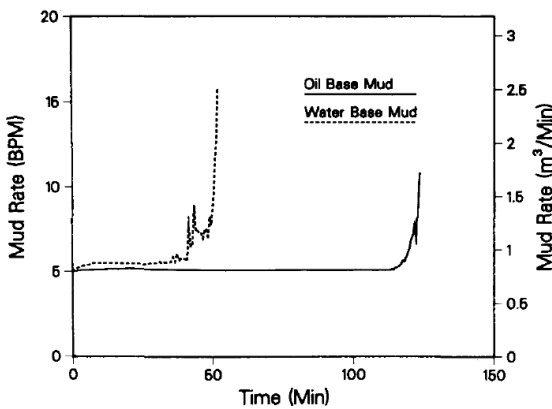


Figure 3. Return flow [3].

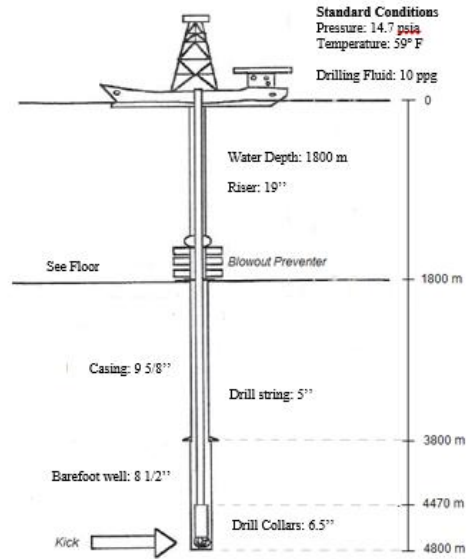


Figure 4. Scenario studied – input data.

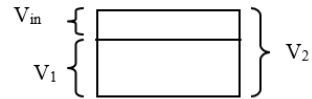


Figure 5. Drilling fluid cell. V_2 is the volume of the cell after a certain amount of gas having dissolved in it. V_1 is the volume of the cell with no dissolved gas.

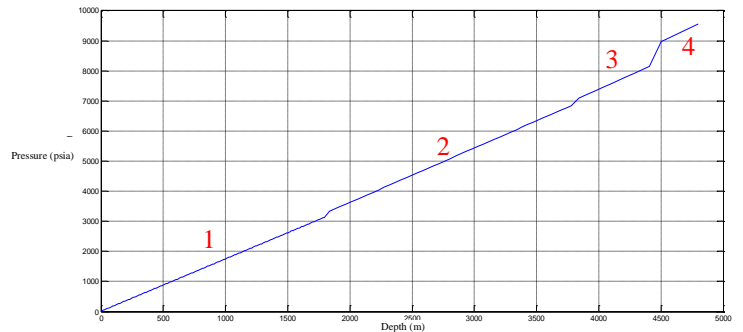


Figure 6. Pressure profile.

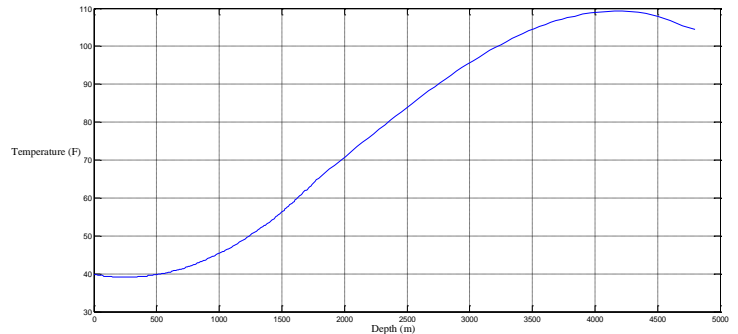


Figure 7. Temperature profile.

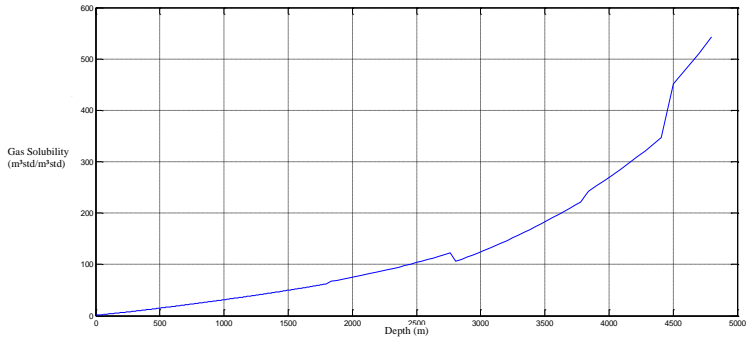


Figure 8. Gas solubility profile.

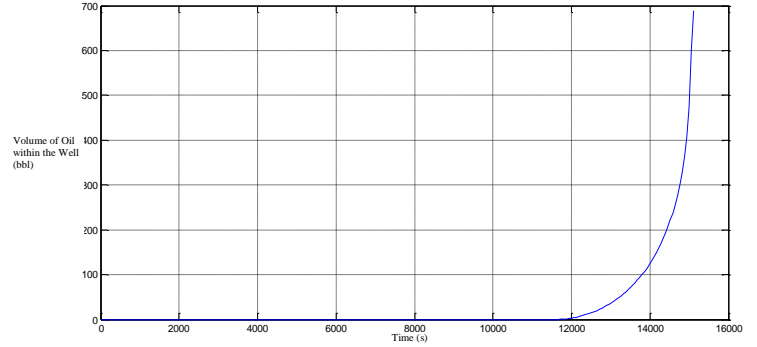


Figure 12. Free gas in the well.

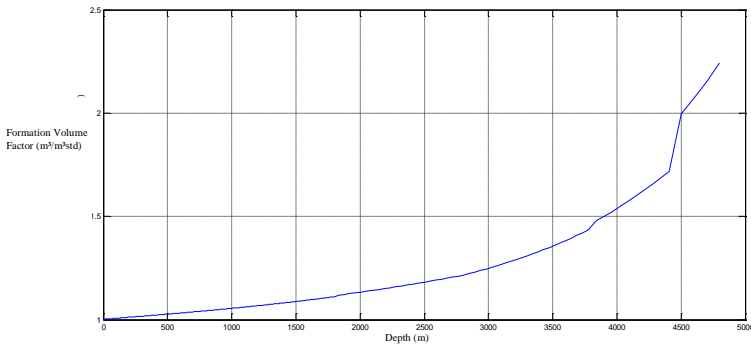


Figure 9. Formation volume factor profile

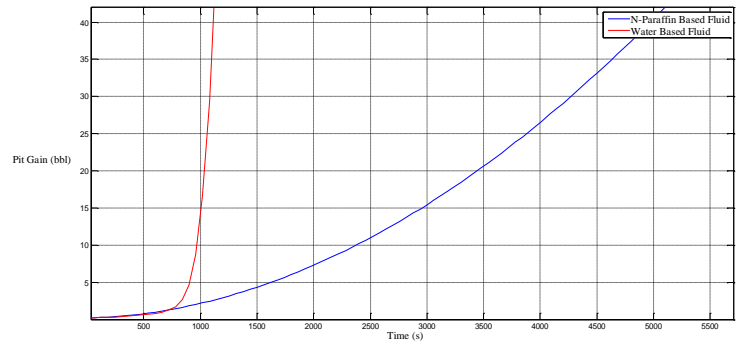


Figure 13. Pit gain – figure amplified in the region of interest.

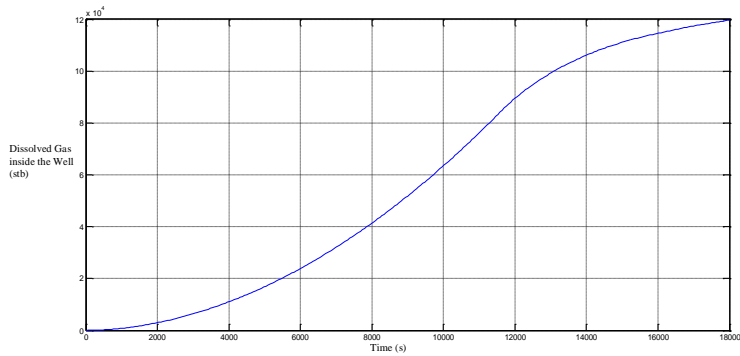


Figure 10. Dissolved gas in the well.

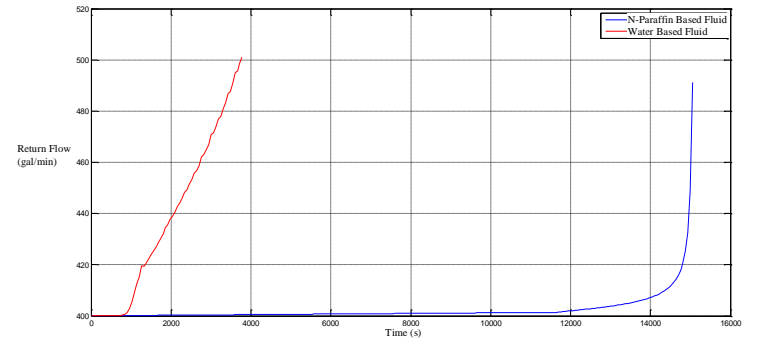


Figure 14. Return flow.

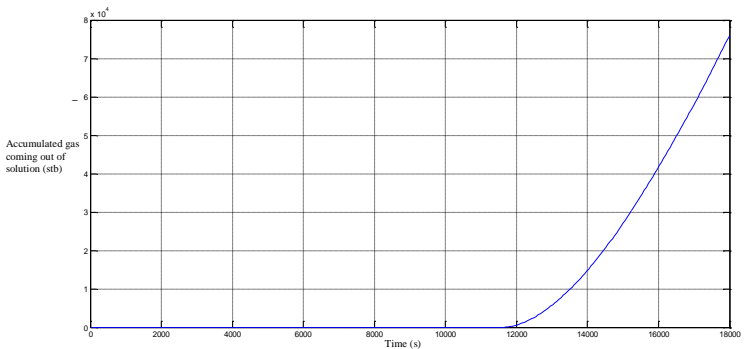


Figure 11. Accumulated gas coming out of solution.

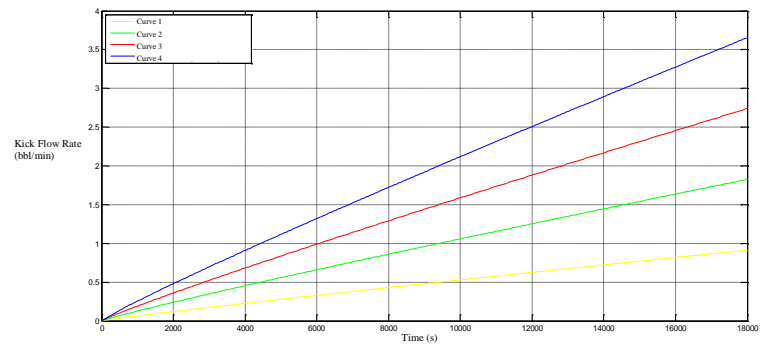


Figure 15: Kick flow rate curves, varying from very low to high.